Performance Comparison of Downlink Capacity Improvement Schemes: Orthogonal Code-Hopping Multiplexing Versus Multiple Scrambling Codes

Bang Chul Jung, *Member, IEEE*, Sung Soo Cho, and Dan Keun Sung, *Senior Member, IEEE*

***Abstract*—In this paper, we compare the performance of two downlink capacity-improvement schemes based on orthogonal code-hopping multiplexing (OCHM) and multiple scrambling codes (MSCs). Both OCHM and MSC systems have been proposed to overcome a code-limitation problem in a code division multiple access (CDMA) downlink. We mathematically analyze the user capacity in a general form, considering various factors such as user activity, spreading factor, amount of transmission symbol energy that is allocated to common control channels, amount of outer-cell interference, orthogonality factor, and sectorization factor. Numerical examples show that the capacity gain of the OCHM-based system increases as the other-cell interference decreases and the channel activity decreases. Thus, the OCHM-based system is a more effective scheme than the MSC-based system, considering that a code-limited situation more frequently occurs in the case of low other-cell interference and low channel activity. However, the OCHM-based system is more sensitive to the orthogonality factor.**

***Index Terms*—Downlink power allocation, multiple scrambling codes (MSCs), orthogonal code hopping multiplexing (OCHM), user capacity.**

I. Introduction

PACKET-TYPE services such as Hypertext Transfer Protocol, File Transfer Protocol, and Wireless Application Protocol have gradually increased and may become dominant in future wireless communication systems. In contrast to voice traffic, these packet-based services have different characteristics. They exhibit high burstiness with low activity, and this packet-based traffic is, in general, more concentrated on a downlink, because mobile users often demand information from servers. Based on these characteristics, the demand for downlink code channels will increase for packet-based services in third-generation (3G) and beyond 3G systems [1], [2]. However, orthogonal code allocation/deallocation mechanisms in conventional code division multiple access (CDMA) systems are very inefficient at accommodating this bursty downlink packet-type traffic if code channels are allocated to mobile stations (MSs) by a base station (BS) at each session setup and are released from the connection after each session termination. Many inactive periods of bursty traffic cause a waste of orthogonal code channels, and the increased demand for orthogonal code channels results in a lack of orthogonal codewords (OCs), in spite of the remaining BS power.

On the other hand, the shared-channel-based downlink resource allocation method is known to be a very efficient method for bursty data (delay-tolerant) traffic in wireless communication systems [3]–[7]. However, this technique requires a large amount of feedback information and may not correctly operate in rapidly varying channel environments. Furthermore, techniques that are based on scheduling are appropriate for high-rate data services among a small number of users. If a large number of users demand low-rate data services with low channel activities, then a BS should transmit much signaling information, which includes subcarrier allocation, modulation, and coding format, pending data to specific users, to maintain the connections.

An orthogonal code hopping multiplexing (OCHM) system [8]–[12] has been proposed to accommodate a larger number of MSs with bursty traffic than the number of OCs in a downlink. It uses statistical multiplexing for an orthogonal downlink in direct-sequence CDMA (DS-CDMA) systems. Since each MS communicates with a BS through a given orthogonal code hopping pattern (HP), signaling messages for allocation and deallocation of OCs are not needed during a session. An HP can randomly be generated based on an MS-specific number (e.g., an electronic serial number), and HP collisions among MSs may occur.

When an HP collision among MSs occurs in a conventional frequency hopping spread spectrum system, it is considered an inevitable interference (*hit*), given that all MSs are asynchronous with one another [13]. However, an HP collision in an OCHM system can be detected and controlled by a BS in a synchronous downlink environment. If HP collisions occur, then a BS examines user data that experience HP collisions and determines whether all the user data with the same HP collision are identical. If all the corresponding data are identical, the collision does not need to be controlled, and all the colliding symbols of different users are transmitted with a sum of all symbol energies, which results in an energy gain at the receiver. This effect is termed *synergy* in this context [8]. On the contrary, if all data with the same HP collision are not the same, then all

Manuscript received September 27, 2006; revised July 31, 2007, March 27, 2008, and April 23, 2008. First published May 23, 2008; current version published February 17, 2009. This work was supported in part by the BroMA IT Research Center Project. The review of this paper was coordinated by Prof. R. M. Buehrer.

B. C. Jung is with Korea Advanced Institute of Science and Technology Institute for Information Technology Convergence, Daejeon 305 701, Korea (e-mail: bcjung@cnr.kaist.ac.kr).

S. S. Cho is with the QoS Control Platform Division, KT, Daejeon 305 811, Korea (e-mail: nicecho@kt.com).

D. K. Sung is with the Department of Electrical Engineering and Computer Science, Korea Advanced Institute of Science and Technology, Daejeon 305 701, Korea (e-mail: dksung@ee.kaist.ac.kr).

Digital Object Identifier 10.1109/TVT.2008.926070

the corresponding data symbols are not transmitted during the symbol time. This effect is termed *perforation*. Thus, in OCHM systems, the HP collisions do not cause intracell interference (ICI), but the perforations result in information losses. However, these losses can be recovered by a proper channel coding technique with additional energy. Therefore, HP collisions in OCHM systems also differ from the ICI, which is characterized by a cross-correlation function between non-OCs in the uplink of DS-CDMA systems.

There has been some performance comparison between the shared-channel-based resource allocation scheme and the OCHM-based scheme [14], [15]. Extensive system-level simulation for fair performance comparison was performed [14]. The comparison results show that the OCHM-based scheme yields better performance than the shared-channel-based scheme in terms of packet delay, packet delay variance, and fairness. In addition, it has a system throughput advantage with low- or medium-rate services. On the contrary, for the delay-tolerant traffic, the shared-channel-based scheme outperforms the OCHM-based scheme.

Another method for overcoming the code-limited situation is to use multiple scrambling codes (MSCs) [16]. More MSs can be accommodated than the number of OCs in a downlink by using additional nonorthogonal code sequences. One MSC scheme [17] is specified in the WCDMA system, and another type of MSC, i.e., the quasiorthogonal function [18], is used in the cdma2000 (IS2000) system to enhance the system capacity. The MSC sets are generated by different masks that are multiplied by a Walsh code set. For example, the cdma2000 system specifies four different MSC sets, each of which is generated by a distinct mask. Each mask corresponds to a row in a Walsh matrix of size 256. The masks that the cdma2000 standard selected are optimal, in the sense that they minimize the cross-correlation between the generated MSCs and regular Walsh codes with the same length. In general, the MSC sets are found by exhaustive searches for this purpose [19]–[21]. As the number of MSC sets increases, the inner-cell interference also increases. Thus, it is obvious that the number of available MSC sets should be limited due to the corresponding inner-cell interference. Previous studies [20], [22] focused on how the performance of CDMA systems can be enhanced with MSC sets. However, they did not provide a generalized form of capacity analysis.

In this paper, the user capacity of OCHM- and MSC-based systems is mathematically analyzed, and the merits and demerits of both systems are compared. We analyze the user capacity in a general form, considering various factors such as user activity, spreading factor, amount of transmission symbol energy that was allocated to common control channels, amount of outer-cell interference, orthogonality factor, and sectorization factor. One power control mechanism is also considered, with geometric factors such as propagation loss and shadowing effect. The rest of this paper is organized as follows. In Section II, notations for mathematical analysis are listed. In Sections III and IV, the user capacity of OCHM-based systems and that of MSC-based systems are mathematically analyzed. In Section V, numerical examples of both systems are described. Conclusions are presented in Section VI.

II. Notations for Mathematical Analysis

b	index of a home cell or a home BS;
$(E_b/I_0)_{\mathrm{req}}^{\mathrm{OCHM}}$	required E_b/I_0 for a target bit error rate (BER) or frame error rate (FER) in OCHM-based systems;
$(E_s/I_0)_{\mathrm{req}}^{\mathrm{OCHM}}$	required E_s/I_0 for a target BER or FER in OCHM-based systems;
$(E_b/I_0)_{\mathrm{req}}^{\mathrm{MSC}}$	required E_b/I_0 for a target BER or FER in MSC-based systems;
$(E_s/I_0)_{\mathrm{req}}^{\mathrm{MSC}}$	required E_s/I_0 for a target BER or FER in MSC-based systems;
$E_{s,b\to(i,j,b)}^{(t)}$	transmission symbol energy from BS b to MS(i,j,b);
$E_{s,b}^{(t)}$	total transmission symbol energy of BS b;
$E_{s,\max}^{(t)}$	maximum of transmission symbol energy of BS b;
g	index of adjacent cells or adjacent BSs;
$I_{0,(i,j,b)}$	total interference at MS(i,j,b);
M	number of users in a cell;
M_{cs}	total number of code sets that were allocated to M MSs $(=\lceil M/N_{\mathrm{oc}}\rceil)$;
MS(i,j,b)	MS with the ith code in the jth code set that was allocated in cell b;
N_{adj}	number of adjacent cells;
N_{OC}	number of orthogonal codes in a set;
R_e	radius of a circular cell;
R_c	channel (or forward error correction) code rate of a downlink channel;
$r_{b\to(i,j,b)}$	distance from BS b to MS(i,j,b);
SF	spreading factor;
$u(x)$	unit step function (when $x\geq 0$, the value is 1; otherwise, it is 0);
$\lceil x\rceil$	Smallest integer that is larger than or equal to x;
$\lfloor x\rfloor$	largest integer that is smaller than or equal to x;
$\alpha_{(i,j,b)}$	orthogonality factor that affects MS(i,j,b);
β_{PN}	interference suppression factor that is equal to the autocorrelation of a PN sequence at a nonzero offset;
β_{MSC}	inner-cell interference suppression factor that is the square of the cross correlation between two code sequences in distinct quality-of-service (QoS) sets;
$\Gamma_{b\to(i,j,b)}$	propagation loss from BS b to MS(i,j,b);
γ	propagation loss exponent $(=4)$;
λ	sectorization factor;
$\nu_{(i,j,b)}$	channel activity factor of MS(i,j,b);
$\bar{\nu}$	mean channel activity factor;
μ	modulation order [2 for quaternary phase-shift keying (QPSK), 4 for 16 quadratic-amplitude modulation];
ρ	proportion of power that was allocated to common control channels;
η	power ratio between home BS and other cell BSs $(E_{s,k(k\neq 0)}^{(t)}/E_{s,0}^{(t)})$.

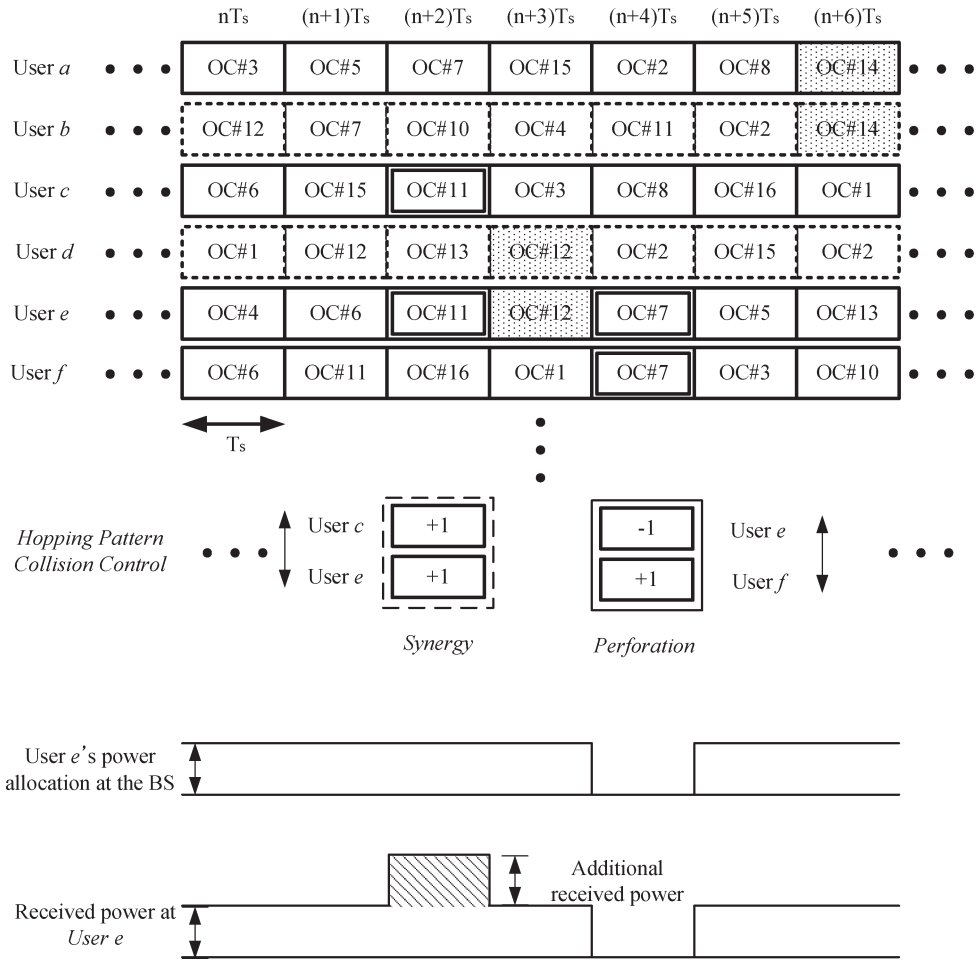

Fig. 1. Operation of an OCHM system.

III. Downlink User Capacity of OCHM-Based Systems

A. OCHM Mechanism, HP Collisions, Perforation, and Synergy

OCHM systems use a synergy and perforation scheme for controlling HP collisions at a BS. Fig. 1 shows the operation of an OCHM-based system that uses a synergy and perforation scheme. It also shows one example of both the transmitted and received power levels for a specific user. The term T_s denotes the symbol time. Each user changes the OC according to a given HP at each symbol time, during which an HP collision may occur. However, most of the users may be inactive because of low channel activities when they demand data services. Users b and d are inactive in Fig. 1, so they follow their HPs during their sessions. In this case, HP collisions between an active user group and an inactive user group do not affect the performance of the active user group. The shaded parts in Fig. 1 indicate this type of collision.

When an HP collision among the active users occurs, a BS compares user data that experience the HP collision and determines whether all user data with the same HP collision are identical. If all the corresponding data are the same, all the corresponding data symbols are transmitted with *synergy*, which results in an energy gain at the receiver. On the other hand, if all data with the same HP collisions are not the same, all the corresponding data symbols are not transmitted. In other words, they are *perforated* during the symbol time. For example, user e experiences a synergy at $(n+2)T_s$ and a perforation at $(n+4)T_s$ (see [8]–[12] for details on the OCHM systems).

If an HP is randomly generated, the HP collision probability of a random-hopping (RH) OCHM-based system is expressed as

$$P_c^{\mathrm{RH}} = 1 - \left(1 - \frac{\bar{v}}{N_{\mathrm{OC}}}\right)^{M-1} \tag{1}$$

where N_{OC} and M indicate the number of orthogonal codes in a set and the number of users in a cell, respectively. For a given mean channel activity $\bar{v}$, P_c^{RH} increases as the number of active users increases. The perforation probability of encoded symbols in the RH OCHM-based systems is written as

$$P_p^{\mathrm{RH}} = 1 - \left(1 - \frac{s-1}{s} \cdot \frac{\bar{v}}{N_{\mathrm{OC}}}\right)^{M-1} \tag{2}$$

where s is the number of symbol locations per dimension [$s = 2$ for binary phase-shift keying (BPSK) and QPSK modulations]. Hence, the synergy probability is given as

$$P_s^{\mathrm{RH}} = P_c^{\mathrm{RH}} - P_p^{\mathrm{RH}}. \tag{3}$$

Recently, we have proposed a new code hopping method, which is called the group-mode hopping (GH) mechanism [23], to mitigate the effect of HP collisions. In the GH mechanism, downlink channels are divided into collisionfree groups (CFGs). There are $\lfloor M/N_{\rm OC} \rfloor$ groups with $N_{\rm OC}$ OCs within each group and one last group with a size of $M - \lfloor M/N_{\rm OC} \rfloor \cdot N_{\rm OC}$ if this size is not equal to zero. $\lfloor x \rfloor$ indicates the largest integer that is smaller than or equal to x. Within a CFG, the exclusively assigned HPs do not collide with each other. In other words, the GH mechanism prevents intragroup collisions. Thus, HP collisions occur only among users in different CFGs. If we use a GH mechanism, then (1)–(3) can be replaced, respectively, as

$$P_c^{\rm GH} = \frac{M - N_{\rm last}}{M}\left\{1 - (1-\bar{\nu})^{\left\lfloor \frac{M}{N_{\rm OC}} \right\rfloor - 1} \cdot \left(1 - \frac{\bar{\nu} N_{\rm last}}{N_{\rm oc}}\right)\right\} + \frac{N_{\rm last}}{M}\left\{1 - (1-\bar{\nu})^{\left\lfloor \frac{M}{N_{\rm OC}} \right\rfloor}\right\} \tag{4}$$

$$P_p^{\rm GH} = \frac{M - N_{\rm last}}{M}\left\{1 - \left(1 - \frac{s-1}{s}\cdot\bar{\nu}\right)^{\left\lfloor \frac{M}{N_{\rm OC}} \right\rfloor - 1} \cdot \left(1 - \frac{s-1}{s}\cdot\frac{\bar{\nu} N_{\rm last}}{N_{\rm OC}}\right)\right\} + \frac{N_{\rm last}}{M}\left\{1 - \left(1 - \frac{s-1}{s}\cdot\bar{\nu}\right)^{\left\lfloor \frac{M}{N_{\rm OC}} \right\rfloor}\right\} \tag{5}$$

$$P_s^{\rm GH} = P_c^{\rm GH} - P_p^{\rm GH} \tag{6}$$

where $N_{\rm last}$ is the number of users in the last CFG.

B. POM

We define a received signal model to analyze the BER of an OCHM system in this section. As we have noted, HP collisions between active users result in information losses, and the BER increases. Thus, we should analyze the BER performance according to the HP collision probability to analyze the system performance. We consider the perforation effect in this model. The received signal model of a BPSK symbol in an additive white Gaussian noise (AWGN) channel is expressed as

$$Y = \begin{cases} t_1 \sim N(0, \sigma^2), & \text{for a perforation} \\ t_2 \sim N(\sqrt{E_s}, \sigma^2), & \text{otherwise} \end{cases} \tag{7}$$

where we assume that a positive symbol is transmitted, and its received symbol energy is . In addition, $x \sim N(m, \sigma^2)$ represents that x is a Gaussian random variable with mean m and variance σ^2. We call this model a perforation-only model (POM), because it considers a perforation effect when HP collisions occur. The distribution function of POM is obtained as

$$F_Y(y) = G\left(\frac{y}{\sigma}\right)\cdot P_p + G\left(\frac{y-\sqrt{E_s}}{\sigma}\right)\cdot(1-P_p) \tag{8}$$

where

$$G\left(\frac{x-m}{\sigma}\right) = \int_{-\infty}^{x} \frac{1}{\sqrt{2\pi\sigma^2}} e^{-(x-m)^2/2\sigma^2} dx.$$

Therefore, the probability density function of the received signal in OCHM systems is given as

$$f_Y(y) = P_p \cdot \frac{1}{\sqrt{2\pi\sigma^2}} e^{-y^2/2\sigma^2} + (1-P_p)\cdot\frac{1}{\sqrt{2\pi\sigma^2}} e^{-(y-\sqrt{E_s})^2/2\sigma^2} \tag{9}$$

where the received signal follows the POM. This POM provides a lower bound of the BER performance of OCHM systems. Furthermore, the POM maintains the consistency according to the distance between MSs and a BS, since the perforation effect is not dependent on the relative distance. The BER performance based on this POM provides the overall system performance, regardless of the location of MSs for a given HP collision probability. If we consider the synergy effect, then the BER performance of a user varies according to the relative distance of the user, since the quantity of the additional energy at the receiver due to synergy is determined by the distances between a BS and code-collision users if the OCHM-based system uses a power control scheme. Statistically, users near a BS have a more energy gain than those at the cell boundary. The energy gain at the receiver due to the synergy scheme is too complex to analyze in OCHM-based systems. Therefore, we use this POM for the BER performance analysis in the rest of this paper.

C. BER Performance of an OCHM System

We use the POM to investigate the coded bit error probability of the OCHM system with a convolutional code (CC). The CC is one of the most commonly used channel coding schemes in wireless communication systems. We assume that a BPSK modulation is used for transmitting symbols over an AWGN channel with one-sided power spectral density N_0. For a soft-decision Viterbi decoder, the event and bit error probability bounds in OCHM systems with a CC are expressed as [24], [25]

$$P_{e,\rm CC}^{\rm OCHM} < \sum_{d=d_{\rm free}}^{\infty} A_d \sum_{i=0}^{d} \binom{d}{i} (1-P_p)^i P_p^{d-i} Q\left(\sqrt{\frac{2i^2 R_c E_b}{dN_0(1-P_p)}}\right) \tag{10}$$

$$P_{b,\rm CC}^{\rm OCHM} < \sum_{d=d_{\rm free}}^{\infty} B_d \sum_{i=0}^{d} \binom{d}{i} (1-P_p)^i P_p^{d-i} Q\left(\sqrt{\frac{2i^2 R_c E_b}{dN_0(1-P_p)}}\right) \tag{11}$$

where A_d and B_d are determined by the encoder structure. The term $d_{\rm free}$ indicates the free distance of the CC.

We now consider turbo codes (TCs) as a channel coding scheme for an OCHM system. The original concept of TCs

was introduced in [26], and the theoretical justification for the performance of TCs was provided by Benedetto and Montorsi in [27], [28]. TCs yield an excellent performance, which is very close to a Shannon limit at low and medium E_b/N_0 values. However, the TC performance curve shows a slope change at high E_b/N_0 values if the codefree distance is small. This phenomenon is called an *error floor*. In fact, the BER performance of the TC at low or medium E_b/N_0 values is hard to analyze, and most of the previous studies on the TC performance assumed relatively high E_b/N_0 values, which indicate an error floor region. Under this assumption, the bit error probability of the TCs is expressed as [27]

$$P_{b,\mathrm{TC}} \approx \frac{W_{\mathrm{free}}}{L_{\mathrm{frame}}} \cdot Q\left(\sqrt{\frac{2d_{\mathrm{free}}R_cE_b}{N_0}}\right) \tag{12}$$

where L_{frame} and W_{free} indicate the frame length and the information bit multiplicity of the free distance, respectively. Equation (12) is based on the fact that the code performance for high E_b/N_0 values essentially coincides with a union bound that was truncated to the contribution of the free distance, which is similar to the CC case. Note that the BER performance of the TC is also determined by the information block length, the free distance, and its multiplicity. Furthermore, the interleaver structure is the most important component for a good performance in the TC, since it determines the free distance and its multiplicity.

We need to compute the first several terms of the distance spectrum to produce a more accurate estimate, particularly at the E_b/N_0 values where a slope change occurs. If we now evaluate the expression of the truncated union bound by considering the contribution of several terms of its distance spectrum, we obtain the truncated union bound as follows:

$$\mathrm{UB}(l) \approx \frac{W_{\mathrm{free}}}{L_{\mathrm{frame}}} \cdot Q\left(\sqrt{\frac{2d_{\mathrm{free}}R_cE_b}{N_0}}\right) + \sum_{i=2}^{l} \frac{W_i}{L_{\mathrm{frame}}} \cdot Q\left(\sqrt{\frac{2d_iR_cE_b}{N_0}}\right) \tag{13}$$

where d_i and W_i indicate the ith distance and the bit multiplicity of the distance spectrum, respectively. For concatenated codes, a small penalty (usually less than 0.5 dB) must be taken into account due to the suboptimality of iterative decoding [29]. However, in (12) and (13), the bit error probability at high E_b/N_0 values is estimated, and its slope is obtained. In most cases, the parameters d_i and W_i are not easy to find, since they are closely related to the interleaver structure. There have been many studies on the calculation of the free distance and its multiplicity of the TCs for a given interleaver [29], [30]. In this paper, we compute the distance spectrum coefficients according to the method in [30].

When a TC is used for OCHM-based systems, we can approximate the bit error probability by using the previous error floor analysis (12) or truncated union bound analysis (13). Basically, the bit error probability analysis of TCs is similar to that of the CC cases, except for the computation of distance spectrum coefficients. Based on the previous analysis of the CC, the bit error probability of TC is expressed as

$$P_{b,\mathrm{TC}}^{\mathrm{OCHM}} \approx \frac{W_{\mathrm{free}}}{L_{\mathrm{frame}}} \times \sum_{i=0}^{d_{\mathrm{free}}} \binom{d_{\mathrm{free}}}{i} (1-P_p)^i P_p^{d_{\mathrm{free}}-i} \times Q\left(\sqrt{\frac{2i^2R_cE_b}{d_{\mathrm{free}}N_0(1-P_p)}}\right) \tag{14}$$

$$\mathrm{UB}^{\mathrm{OCHM}}(l) \approx \sum_{j=1}^{l} \frac{W_j}{L_{\mathrm{frame}}} \times \sum_{i=0}^{d_j} \binom{d_j}{i} (1-P_p)^i P_p^{d_j-i} \times Q\left(\sqrt{\frac{2i^2R_cE_b}{d_jN_0(1-P_p)}}\right) \tag{15}$$

where $d_1 = d_{\mathrm{free}}$, and $W_1 = W_{\mathrm{free}}$.

D. FER Analysis From the BER Performance Analysis

In data communications, FER is an important QoS measure, because even a single bit error in a frame can make the frame useless. A reasonable approximation for calculating the FER of a channel coding scheme is given by

$$\mathrm{FER} \simeq 1 - (1-P_b)^{L_{\mathrm{frame}}} \simeq P_b \cdot L_{\mathrm{frame}} \tag{16}$$

where $P_b (P_b \ll 1)$ and L_{frame} denote the bit error probability of a channel coding scheme and the frame length, respectively.

E. Downlink Power Allocation for the OCHM System

In the OCHM system, the downlink power that is allocated for a specific MS is determined by the perforation probability P_p and the channel environment. The perforation probability varies according to both the number of users in a cell and the user activity at a specific time. Previous work only considered the mean perforation probability according to the number of MSs in a cell. However, the perforation probability of each MS is different from each other. Some MSs have lower or higher perforation probabilities than others at a given time. A BS can know the exact number of perforated symbols in downlink frames that were delivered to MSs at the time. Through the BER performance analysis shown in Section III-C, the BS can determine the allocated power for a specific MS in the downlink. If the BER or FER performance analysis does not exist, then a link-level simulation result is required in each case.

The additional required E_b/I_0 at an MS due to the perforation can be expressed as

$$\Delta(E_b/I_0) = f(\zeta_{\mathrm{req}}, P_p) - f(\zeta_{\mathrm{req}}, 0) \tag{17}$$

where ζ_{req} and $f(A, B)$ denote the required FER at the receiver and the function of the required E_b/I_0 at the MS for $\zeta_{\mathrm{req}} = A$ and $P_p = B$, respectively, as derived from (11), (15), and (16). The last term in (17) indicates the required E_b/I_0 for $P_p = 0$, which is the required E_b/I_0 in conventional CDMA systems.

Therefore, the required E_b/I_0 for a given P_p and ζ_{req} in OCHM-based systems is given by

$$\left(\frac{E_b}{I_0}\right)_{\text{req}}^{\text{OCHM}} = f(\zeta_{\text{req}}, P_p) = f(\zeta_{\text{req}}, 0) + \Delta\left(\frac{E_b}{I_0}\right). \quad (18)$$

The allocated symbol power for a specific MS at the BS is determined as

$$P_T = \frac{f(\zeta_{\text{req}}, P_p) \cdot \mu R_c \cdot I_{0,(i,j,b)}}{T_s \cdot \Gamma_{b\to(i,j,b)}} \quad (19)$$

where T_s, R_c, and μ denote the symbol time, channel code rate, and modulation order, respectively. Let MS(i,j,b) be the MS with the ith code in the jth code set that was allocated in cell b, where b indicates the index of a home cell or a home BS. $I_{0,(i,j,b)}$ indicates the total interference at MS(i,j,b). There is one code set in OCHM-based systems; thus, $j=1$ in (19). As P_p increases, the required energy at receiver $f(\zeta_{\text{req}}, P_p)$ increases, and the allocated power P_T also increases.

The total interference at MS(i,j,b) consists of inner-cell interference due to multipath signals $I_{\text{ic},(i,j,b)}^{\text{MP}}$, outer-cell interference due to interfering signals from adjacent cells $I_{\text{oc},(i,j,b)}$, and AWGN N_0 in OCHM-based systems. Thus, the total interference at MS(i,j,b) is expressed as

$$I_{0,(i,j,b)} = I_{\text{ic},(i,j,b)}^{\text{MP}} + I_{\text{oc},(i,j,b)} + N_0. \quad (20)$$

1) Inner-Cell Interference at MS(i,j,b) Due to Multipaths: A partial loss in orthogonality due to multipath signals induces inner-cell interference at all MSs. We represent the orthogonality factor by using α. The factor α is defined with a range from 0 (i.e., complete loss of orthogonality among the different signals) to 1 (i.e., perfect orthogonality among different signals). For example, a profile with almost-perfect orthogonality $(0.98<\alpha<1)$ is used to model line-of-sight channels, a profile with good orthogonality $(0.75<\alpha<0.98)$ represents Pedestrian A channels, and all other profiles represent Vehicular A [32]. Considering the factor α, the interference at MS(i,j,b) due to multipaths is expressed as

$$\begin{aligned} I_{\text{ic},(i,j,b)}^{\text{MP}} &= \beta_{\text{PN}}\left(1-\alpha_{(i,j,b)}\right) E_{s,b}^{(t)} \cdot \Gamma_{b\to(i,j,b)} \\ &= \beta_{\text{PN}}\left(1-\alpha_{(i,j,b)}\right)\left\{\rho E_{s,\max}^{(t)} + \frac{1}{\lambda}\sum_{(x,y,b)} \nu_{(x,y,b)} \right. \\ &\qquad \left. \times E_{s,b\to(x,y,b)}^{(t)}\right\} \cdot \Gamma_{b\to(i,j,b)} \end{aligned} \quad (21)$$

where β_{PN}, $E_{s,b}^{(t)}$, and $\Gamma_{b\to(i,j,b)}$ denote the interference suppression factor, the total transmission symbol energy of BS b, and the propagation loss from BS b to MS(i,j,b), respectively. Moreover, ρ, $E_{s,\max}^{(t)}$, λ, and $\nu_{(x,y,b)}$ represent the proportion of power that was allocated to common control channels, the maximum of transmission symbol energy of BS b, the sectorization factor, and the channel activity factor of MS(i,j,b), respectively. $E_{s,b\to(i,j,b)}^{(t)}$ indicates the transmission symbol energy from BS b to MS(i,j,b).

2) Outer-Cell Interference at MS(i,j,b): We can model outer-cell interference as shown in (22). $I_{\text{oc},(i,j,b)}$ has a maximum value when six adjacent BSs transmit signals with their maximum power, whereas $I_{\text{oc},(i,j,b)}$ has a minimum value when neighboring BSs transmit only common control channel signals. Here, β_{PN} is set to $1/N_{\text{oc}}$ [34], i.e.,

$$\begin{aligned} I_{\text{oc},(i,j,b)} &= \beta_{\text{PN}} \cdot \sum_{g\neq b} E_{s,g}^{(t)} \cdot \Gamma_{g\to(i,j,b)} \\ &= \beta_{\text{PN}} \cdot \sum_{g\neq b}\left\{\rho E_{s,\max}^{(t)} + \frac{1}{\lambda}\sum_{(x,y,g)} \nu_{(x,y,g)} \sum_{(x,y,g)} E_{s,g\to(x,y,g)}^{(t)}\right\} \\ &\quad \cdot \Gamma_{g\to(i,j,b)} \end{aligned} \quad (22)$$

where g denotes the index of adjacent cells or adjacent BSs.

F. User-Capacity Analysis

OCHM was proposed to accommodate more MSs than the number of codewords in the downlink of CDMA systems. There exists no code limitation because of using random code HPs instead of fixed codes so that the user capacity is not limited by the number of codes in a cell. It is limited by only the maximum transmission power of a BS. The downlink transmission power of a BS causes interference to adjacent cells, so the total downlink transmission power should be limited to a specific value $P_{\max}$. In other words, we can say that the total transmission symbol energy $E_{s,b}^{(t)}$ of a BS b is limited to the maximum total transmission symbol energy $E_{s,\max}^{(t)} = P_{\max} \cdot T_s$. Dividing $E_{s,b}^{(t)}$ into two parts of downlink common control channels and downlink user traffic channels, the constraint for the total transmission symbol energy of BS b is written as

$$E_{s,b}^{(t)} = \rho E_{s,\max}^{(t)} + \sum_{(i,j,b)} \nu_{(i,j,b)} E_{s,b\to(i,j,b)}^{(t)} \le E_{s,\max}^{(t)}. \quad (23)$$

Equation (23) is a main requirement for determining the power capacity in CDMA systems.

By using (20)–(22), the transmission symbol energy in the OCHM-based system can be derived as

$$E_{s,b}^{(t)} = \rho E_{s,\max}^{(t)} + \bar{\nu} \cdot S \cdot \sum_{n=1}^{M_b^p}\left(\Phi_1 + \Omega_{(n,1,b)}\right) \le E_{s,\max}^{(t)} \quad (24)$$

where

$$\begin{aligned} S &= \frac{1}{1 - M\cdot\phi_1} \\ \phi_1 &= \beta_{\text{PN}}(1-\bar{\alpha})\left(\frac{E_b}{I_0}\right)_{\text{req}}^{\text{OCHM}} \times \frac{\bar{\nu}}{\lambda \cdot R_c \cdot \mu} \\ \Phi_1 &= \beta_{\text{PN}}(1-\bar{\alpha})\left(\frac{E_b}{I_0}\right)_{\text{req}}^{\text{OCHM}} \times \frac{\rho E_{s,\max}^{(t)}}{R_c \cdot \mu} \\ \Omega_{(n,1,b)} &= \beta_{\text{PN}}\left\{\frac{1}{\lambda}\sum_{g=1}^{N_{\text{adj}}} E_{s,g}^{(t)} \Gamma_{g\to(n,1,b)} + N_0\right\} \\ &\quad \times \left(\frac{E_b}{I_0}\right)_{\text{req}}^{\text{OCHM}} \times \frac{\Gamma_{b\to(n,1,b)}^{-1}}{R_c \cdot \mu} \end{aligned}$$

where N_{adj} indicates the number of adjacent cells. In OCHM-based systems, P_p increases as the number of users in a cell increases, and the required E_b/N_0 at an MS $(E_b/I_0)_{\mathrm{req}}^{\mathrm{OCHM}}$ increases as P_p increases. Thus, the transmitted energy for the MS increases, and the user capacity can be limited. As we have noted, the required E_b/N_0 at the MS, i.e., $(E_b/I_0)_{\mathrm{req}}^{\mathrm{OCHM}}$, is determined by the channel coding capability that is used in the OCHM-based systems. Furthermore, the perforation probability P_p varies according to HP generation methods. If we use a GH instead of an RH, we can reduce the P_p for a given number of users.

IV. Downlink User Capacity of MSC-Based Systems

In MSC-based systems, the total interference at MS(i,j,b) consists of inner-cell interference due to multipath signals $\widetilde{I_{\mathrm{ic},(i,j,b)}^{\mathrm{MP}}}$, another inner-cell interference due to a partial loss in orthogonality among MSC sets $I_{\mathrm{ic},(i,j,b)}^{\mathrm{MSC}}$, outer-cell interference due to interfering signals from adjacent cells $I_{\mathrm{oc},(i,j,b)}$, and AWGN N_0, i.e.,

$$I_{0,(i,j,b)} = \widetilde{I_{\mathrm{ic},(i,j,b)}^{\mathrm{MP}}} + I_{\mathrm{ic},(i,j,b)}^{\mathrm{MSC}} + I_{\mathrm{oc},(i,j,b)} + N_0. \tag{25}$$

The other-cell interference and additive noise in (25) are the same as those of OCHM-based systems.

A. Inner-Cell Interference at MS(i,j,b) Due to Multipath Signals

Let M_{cs} be the total number of code sets allocated to M MSs $(=\lceil M/N_{\mathrm{oc}}\rceil)$, where $\lceil x\rceil$ represents the smallest integer that is larger than or equal to x. Inner-cell interference due to multipath signals at MS(i,j,b) arises among users in the same MSC set in MSC-based systems, since the signal of users in a different MSC set affects the inner-cell interference, regardless of multipath fading. For $1 \le j \le M_{\mathrm{cs}}-1$, the inner-cell interference due to multipath signals is expressed as

$$\begin{aligned}\widetilde{I_{\mathrm{ic},(i,j,b)}^{\mathrm{MP}}} &= \beta_{\mathrm{MSC}}\left(1-\alpha_{(i,j,b)}\right)E_{s,b}^{(t)}\Gamma_{b\to(i,j,b)} \\ &= \beta_{\mathrm{MSC}}\left(1-\alpha_{(i,j,b)}\right) \\ &\quad\times\left\{\rho E_{s,\max}^{(t)} + \frac{1}{\lambda}\sum_{x=1}^{N_{\mathrm{OC}}}\nu_{(x,j,b)}E_{s,b\to(x,j,b)}^{(t)}\right\}\Gamma_{b\to(i,j,b)}\end{aligned} \tag{26}$$

where β_{MSC} denotes the inner-cell interference suppression factor. For $j = M_{\mathrm{cs}}$, the inner-cell interference due to multipath signals is expressed as

$$\begin{aligned}\widetilde{I_{\mathrm{ic},(i,j,b)}^{\mathrm{MP}}} &= \beta_{\mathrm{MSC}}(1-\alpha_{(i,M_{\mathrm{cs}},b)})\left\{\rho E_{s,\max}^{(t)}\right. \\ &\quad\left. + \frac{1}{\lambda}\sum_{x=1}^{N_{\mathrm{last}}}\nu_{(x,M_{\mathrm{cs}},b)}E_{s,b\to(x,M_{\mathrm{cs}},b)}^{(t)}\right\}\Gamma_{b\to(i,M_{\mathrm{cs}},b)}\end{aligned} \tag{27}$$

where N_{last} indicates the number of users that belong to the last MSC set.

B. Inner-Cell Interference at MS(i,j,b) Due to MSC

All code sequences within the same set are orthogonal to one another, whereas the cross-correlation between two code sequences of distinct sets is not zero. Here, it is meaningful to derive the lower bound for the maximum absolute cross correlation. Let N_{oc} be the size of a Walsh code. In addition, let $\mathbf{c} = (c_1, c_2, \ldots, c_{N_{\mathrm{oc}}})$ be any vector with symbols that are complex roots of unity. Then, the lower bound for the maximum absolute cross correlation $|R_{\mathbf{c},\mathbf{w_j}}|$ between $\mathbf{c}$ and any Walsh code $\mathbf{w_j}$ in the Walsh code set $W_{N_{\mathrm{oc}}}$ is given by [22]

$$\max\left\{|R_{\mathbf{c}}\mathbf{w_j}| : \mathbf{c} \notin W_{N_{\mathrm{oc}}}\mathbf{w_j} \in W_{N_{\mathrm{oc}}}\right\} \ge \frac{1}{\sqrt{N_{\mathrm{oc}}}}.$$

This bound also holds for the correlation between any two MSC sets. Thus, to minimize the interference effect, it would be desirable to select a proper masking function such that the correlation between the MSC set and the Walsh code satisfies the above-mentioned equality bound.

Let the square of this statistical cross correlation be β_{MSC} and consider the relationship among code sequences. Then, we can classify the inner-cell interference due to nonzero cross correlation among code sequences into two cases, as shown in the following:

– For $1 \le j \le M_{\mathrm{cs}} - 1$

$$\begin{aligned}I_{\mathrm{ic},(i,j,b)}^{\mathrm{MSC}} &= \beta_{\mathrm{MSC}}\frac{1}{\lambda}\sum_{y=1,y\neq j}^{M_{\mathrm{cs}}}\sum_{x=1}^{N_{\mathrm{OC}}}\bar{\nu}E_{s,b\to(x,y,b)}^{(t)}\Gamma_{b\to(i,j,b)} \\ &\quad+\beta_{\mathrm{MSC}}\frac{1}{\lambda}\sum_{x=1}^{N_{\mathrm{last}}}\bar{\nu}E_{s,b\to(x,M_{\mathrm{cs}},b)}^{(t)}\Gamma_{b\to(i,j,b)}.\end{aligned} \tag{28}$$

– For $j = M_{\mathrm{cs}}$

$$\begin{aligned}I_{\mathrm{ic},(i,M_{\mathrm{cs}},b)}^{\mathrm{MSC}} &= \beta_{\mathrm{MSC}}\frac{1}{\lambda}\cdot\sum_{y=1}^{M_{\mathrm{cs}}-1}\sum_{x=1}^{N_{\mathrm{OC}}}\bar{\nu}E_{s,b\to(x,y,b)}^{(t)} \\ &\quad\times\Gamma_{b\to(i,M_{\mathrm{cs}},b)}.\end{aligned} \tag{29}$$

C. Downlink Power Allocation for MSC Systems

In this analysis, we assume that the transmission power is perfectly controlled. The BS adjusts the transmission power so that MSs receive their signal with a given $(E_b/I_0)_{\mathrm{req}}^{\mathrm{MSC}}$. The required transmission symbol energy from BS b to MS(i,j,b) is expressed as

$$\begin{aligned}E_{s,b\to(i,j,b)}^{(t)} &= I_{0,(i,j,b)}\left(\frac{E_s}{I_0}\right)_{\mathrm{req}}^{\mathrm{MSC}}\Gamma_{b\to(i,j,b)}^{-1} \\ &= \left[I_{\mathrm{ic},(i,j,b)}^{\mathrm{MSC}} + \widetilde{I_{\mathrm{ic},(i,j,b)}^{\mathrm{MP}}} + I_{\mathrm{oc},(i,j,b)} + N_0\right] \\ &\quad\times\left(\frac{E_s}{I_0}\right)_{\mathrm{req}}^{\mathrm{MSC}}\Gamma_{b\to(i,j,b)}^{-1}.\end{aligned} \tag{30}$$

The downlink power that was allocated to MS(i,j,b) is given $E_{s,b\to(i,j,b)}^{(t)}/T_s$, where T_s indicates the symbol time. As the number of users in a cell increases, the inner-cell interference

due to non-OCs $I^{\mathrm{MSC}}_{\mathrm{ic},(i,j,b)}$ increases, and the required downlink power for a single user at the BS also increases.

D. User-Capacity Analysis

Using (25)–(30), the constraint for the total transmission symbol energy of BS b in the MSC-based systems can be derived as [33]

$$E^{(t)}_{s,b} = \rho E^{(t)}_{s,\max} + \bar{\nu}\cdot\sum_{n=1}^{M}\Bigg(\Theta_2+\Phi_2 + \Omega_{\left(n-\left(\left\lceil\frac{n}{N_{\mathrm{OC}}}\right\rceil-1\right)N_{\mathrm{OC}},\left\lceil\frac{n}{N_{\mathrm{OC}}}\right\rceil,b\right)}\Bigg)\cdot S_n \le E^{(t)}_{s,\max} \quad (31)$$

where

$$\theta_2 = \beta_{\mathrm{MSC}}\left(\frac{E_s}{I_0}\right)^{\mathrm{MSC}}_{\mathrm{req}}\frac{\bar{\nu}}{\lambda}$$

$$\Theta_2 = \beta_{\mathrm{MSC}}\left(\frac{E_s}{I_0}\right)^{\mathrm{MSC}}_{\mathrm{req}}\rho E^{(t)}_{s,\max}$$

$$\phi_2 = \beta_{\mathrm{PN}}(1-\bar{\alpha})\left(\frac{E_s}{I_0}\right)^{\mathrm{MSC}}_{\mathrm{req}}\frac{\bar{\nu}}{\lambda}$$

$$\Phi_2 = \beta_{\mathrm{PN}}(1-\bar{\alpha})\left(\frac{E_s}{I_0}\right)^{\mathrm{MSC}}_{\mathrm{req}}\rho E^{(t)}_{s,\max}$$

$$\Omega_{(x,y,b)} = \left\{\frac{\beta_{\mathrm{PN}}}{\lambda}\sum_{g=1}^{N_{\mathrm{adj}}}E^{(t)}_{s,g}\Gamma_{g\to(x,y,b)}+N_0\right\}\times\left(\frac{E_s}{I_0}\right)^{\mathrm{MSC}}_{\mathrm{req}}\Gamma^{-1}_{b\to(x,y,b)}. \quad (32)$$

Here, $(E_s/I_0)^{\mathrm{MSC}}_{\mathrm{req}}$ indicates the required (E_s/I_0) for a target BER or FER in MSC-based systems. S_n in (31) is defined as follows:

- For $M_{\mathrm{cs}} = 1$

$$S_n = \frac{1}{1-M\phi_2}, \qquad 1\le n\le M. \quad (33)$$

- For $M_{\mathrm{cs}} \ge 2$

$$S_n = \begin{cases}\frac{1-N_{\mathrm{last}}(\phi_2-\theta_2)}{\Pi}, & 1\le n\le (M_{\mathrm{cs}}-1)N_{\mathrm{OC}}\\ \frac{1-N_{\mathrm{OC}}(\phi_2-\theta_2)}{\Pi}, & (M_{\mathrm{cs}}-1)N_{\mathrm{OC}}+1\le n\le M\end{cases} \quad (34)$$

where

$$\Pi = u(M_{\mathrm{cs}}-2)\left\{(1-N_{\mathrm{OC}}\phi_2)(1-N_{\mathrm{last}}\phi_2)-N_{\mathrm{OC}}N_{\mathrm{last}}\theta_2^2\right\} - u(M_{\mathrm{cs}}-3)\left\{1-N_{\mathrm{last}}(\phi_2-\theta_2)\right\}(M_{\mathrm{cs}}-2)N_{\mathrm{OC}}\theta_2. \quad (35)$$

$u(x)$ represents the unit step function (when $x\ge 0$, its value is 1; otherwise, it is 0). For a given $P_{\max}$ at the BS, the user capacity is limited by the $P_{\max}$. Thus, the user capacity of the MSC-based systems is the maximum number of users in a cell that satisfies (31).

TABLE I
SYSTEM PARAMETERS FOR NUMERICAL EXAMPLES

Parameter	Value	Parameter	Value
ρ	0.2	$E^{(t)}_{s,max}$	$\frac{15\times SF}{1.2288\times 10^6}$ [J]
N_{oc}	64	N_0	$-174\,[dBm]$
R_e	1000[m]	β_{PN}	$\frac{1}{N_{oc}}$
γ	4	β_{QOS}	$\frac{1}{N_{oc}}$
α	$0.7\sim 1$	R_c	$\frac{1}{3}$
N_{adj}	6	μ	2 (QPSK)

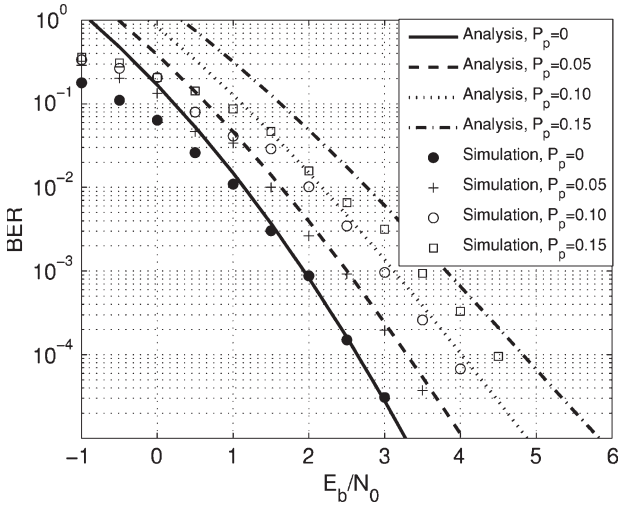

Fig. 2. BER performance of a CC, with $K = 9$, and $R_c = 1/3$.

V. NUMERICAL EXAMPLES

We assume that the maximum transmission symbol energy of a BS is given by $(15\times \mathrm{SF})/(1.2288\times 10^6)$ [J], which is typically used for the cdma2000 system [18]. In addition, we let the cross correlation between two code sequences be $1/\sqrt{N_{\mathrm{oc}}}$, which is the optimal cross-correlation bound, as explained in Section IV-B. Thus, the interference factor due to the introduction of MSCs is $\beta_{\mathrm{MSC}} = (1/\sqrt{N_{\mathrm{oc}}})^2 = 1/N_{\mathrm{oc}}$, which is the square value of the cross correlation. Furthermore, we vary the data channel activity values from 0.1 to 0.5. The system parameters are listed in Table I. λ and R_e represent the propagation loss exponent and the radius of a circular cell, respectively. Under this environment, we analyze the system from the average point of view.

A. BER Performance of OCHM/MSC-Based Systems

Fig. 2 shows the BER performance of a CC in OCHM-based systems. We use a CC with a code rate of 1/3 and a constraint length of 9 ($K = 9$) by using a generator polynomial (557, 663, 711) in octal number, and then, the *free distance* (d_{free}) of the encoder is 18 [35]. The CC that we have introduced was used in the IS-95 uplink system [34]. The solid line indicates the BER performance of the CC in the case of $P_p = 0$, and the broken lines represent (11) in the case of $P_p \ne 0$. The symbols with marks indicate the results of computer simulation. The results of (11) show the upper bound of the simulation results. The BER values increase as the perforation probability increases.

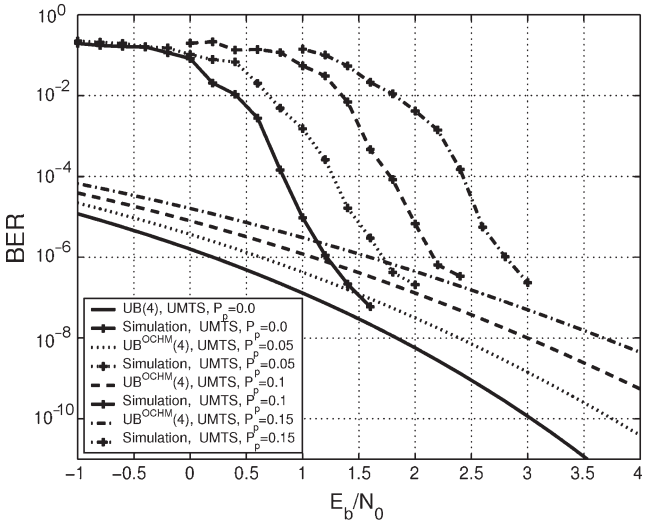

Fig. 3. BER performances of a TC, with $K = 4$, and $R_c = 1/3$.

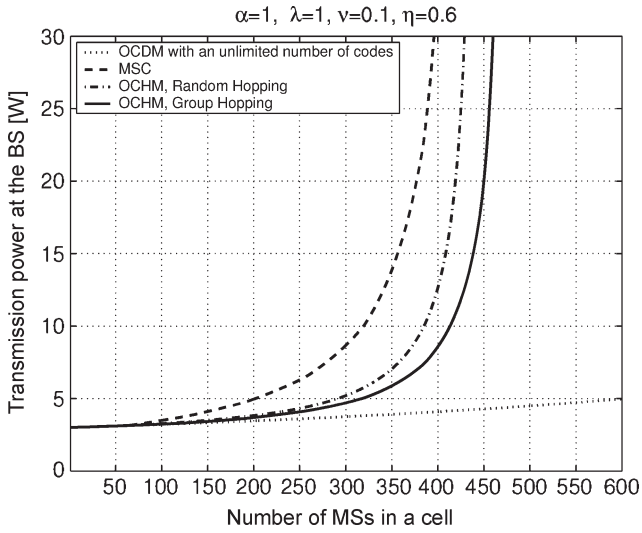

Fig. 4. Downlink transmit power at the BS for varying the number of MSs in four different systems with a CC.

TABLE II
REQUIRED E_b/I_0 AT THE MS ACCORDING TO P_p AND FER_{req}

CC with K=9 and $L_{frame} = 1024$				
ζ_{req}	$P_p = 0.00$	$P_p = 0.05$	$P_p = 0.10$	$P_p = 0.15$
10%	2.63 dB	3.28 dB	4.02 dB	4.82 dB
1%	3.30 dB	4.03 dB	4.89 dB	5.81 dB

TC with K=4 and $L_{frame} = 1024$				
ζ_{req}	$P_p = 0.00$	$P_p = 0.05$	$P_p = 0.10$	$P_p = 0.15$
10%	0.83 dB	1.26 dB	1.77 dB	2.42 dB
1%	1.00 dB	1.40 dB	1.96 dB	2.56 dB

When the P_p value is set to 0.10, the additional required E_b/N_0 is approximately 1.5 dB for a BER value of 10^{-4}. Note that the POM provides the lower bound of the BER performance of OCHM-based systems, since it neglects the synergy effect at the receiver. In fact, the BER performance of OCHM-based systems can be better due to the synergy effect at the receiver.

Fig. 3 shows the BER performance of a TC in OCHM-based systems. In this simulation, we use a TC that was used in a Universal Mobile Telecommunications System [1]. The code rate is 1/3, and the length of information block is 1024. We compute the free distance and coefficients of the first several terms in the distance spectrum according to Garello's algorithm, which was found in [31]. The lines without symbols indicate the result in (15) for the OCHM and the result in (13) for $P_p = 0$. We compute the first four terms in the distance spectrum. The simulation results agree with the analytical ones for high E_b/N_0 values, with a slight difference of about 0.5 dB, which is caused by a suboptimal iterative decoding scheme that was used in the decoder. If the perforation probability is set to 0.15, then the additional required E_b/N_0 at the receiver is about 1.5 dB for a BER value of 10^{-6}. If the required BER is lower than 10^{-6}, then the TC may be inefficient, since it reaches the error floor region, and the slopes of BER performance decrease.

Table II summarizes the required E_b/I_0 of a CC and a TC for varying values of ζ_{req} and P_p. As we have noted, the required E_b/N_0 values increase as P_p increases, and a BS should allocate more power to MSs with large values of P_p. More allocated power to MSs can limit the power capacity. Therefore, the channel coding scheme that was used for the OCHM is a key factor that affects the OCHM performance. If an MS requires larger power than a limit due to its perforation, the BS needs to perform an appropriate admission control scheme to save power consumption.

In the MSC systems, ICI can occur between users that utilize the orthogonal code in the distinct scrambling code set. The interference due to MSCs can be modeled as a Gaussian noise, and it does not affect the BER performance. It only increases the interference quantity at the MS. Thus, the required E_b/N_0 for a given BER requirement does not vary according to the number of users. Thus, the required E_b/I_0 in the MSC-based systems is the same as that of the conventional CDMA systems in the case of the BER graph, where $P_p = 0$ in Figs. 2 and 3.

B. Required Power at the BS of Each System

Fig. 4 shows the downlink transmit power at the BS for varying the number of MSs in a cell for four different systems with a CC: 1) orthogonal code division multiplexing with an unlimited number of codes (i.e., the ideal case); 2) an MSC system; 3) an RH-based OCHM; and 4) a GH-based OCHM. The term η represents the power ratio between a home BS and a neighboring cell BS. All systems require more power at the BS as the number of MSs in a cell increases. The OCHM-based system can be operated in either a GH hopping or RH. If we use the GH, the performance of the OCHM system can be improved. In the MSC-based system, if the number of MSs in a cell is equal to 350, the required power at the BS is larger than 13 W, whereas it is approximately 6 W in the OCHM-based system with a GH. Therefore, the OCHM-based system yields better performance than the MSC-based system. The dotted line in Fig. 4 represents the performance of the system that has an unlimited number of orthogonal codes. In this system, there exist no code limitation in the downlink; thus, it does not induce any inner-cell interference and additional energy at the MS.

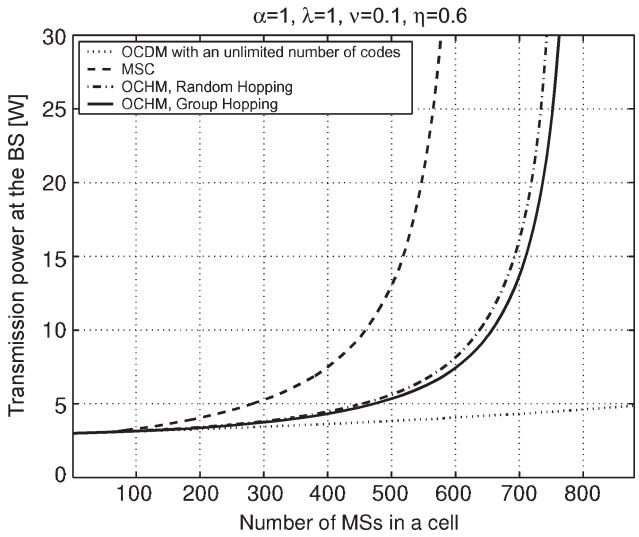

Fig. 5. Downlink transmit power at the BS for varying the number of MSs in four different systems with a TC.

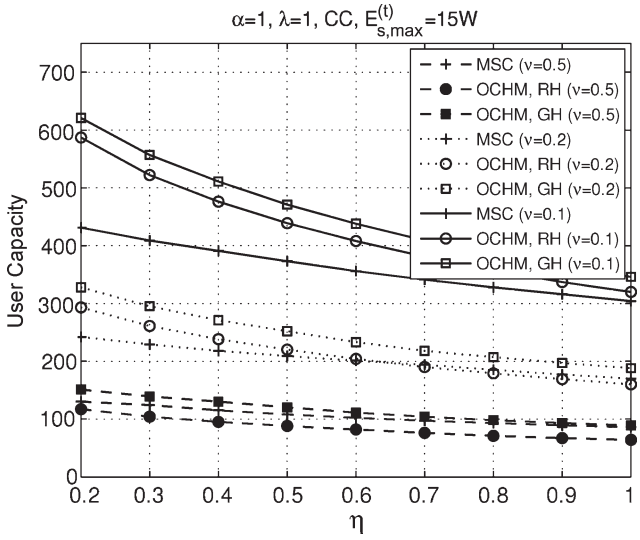

Fig. 6. Downlink user capacity comparison for varying other-cell interference η and activity ν with a CC.

Fig. 5 shows another example of the downlink transmit power at the BS for four different systems with a TC [1]. If we use the TC as a channel coding scheme, the performance of the OCHM-based system can be improved, since additional energy at the MS due to symbol perforations decreases.

C. User Capacity Comparison

Fig. 6 shows the user capacity of the MSC-based system and that of the OCHM-based system for varying the other-cell interference (η) and channel activity. We use a CC as a channel coding scheme. If the channel activity is set to 0.5 like a voice service, the MSC-based system yields better performance than the OCHM-based system with RH patterns. However, as the channel activity decreases, the OCHM-based system with RH patterns yields better performance than the MSC-based system. The OCHM-based system relatively has a larger capacity than the MSC-based system when other-cell interference is small.

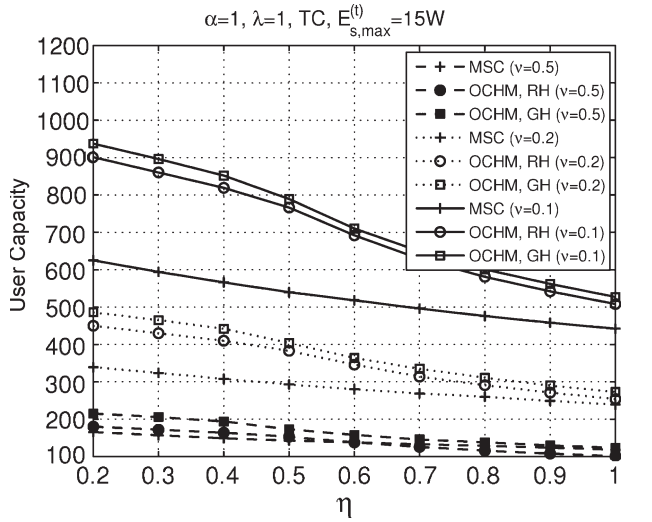

Fig. 7. Downlink user capacity comparison for varying other-cell interference η and activity ν with a TC.

A code-limited situation occurs more frequently when the channel activity is low, and other-cell interference is small [11]; therefore, the OCHM-based system is more effective than the MSC-based system. When the other-cell interference is large or the channel activity is high, the power capacity may be smaller than the code capacity, i.e., the maximum number of available codes in a cell. Furthermore, if we use the OCHM-based system with GH, the OCHM-based system is better than the MSC-based system, regardless of the channel activity. Note that the user capacity of the OCHM-based system with a GH is equal to 438 when $\eta = 0.6$, and it is much larger than a code limit of 64 in the conventional CDMA systems.

Fig. 7 shows the downlink user capacity of the MSC-based system and that of the OCHM-based system when a TC is used as a channel code. The OCHM-based system can accommodate more users than the MSC-based system. The OCHM-based system becomes effective as the channel activity decreases. If η is equal to 0.6 and the channel activity is equal to 0.1, then the downlink user capacity of the MSC-based system, the OCHM-based system with RH, and the OCHM-based system with GH is 518, 692, and 789, respectively. The capacity gain of the OCHM-based system over the MSC-based system decreases as η increases.

The capacity gain of the OCHM-based system over the MSC-based system is defined as

$$C_{\text{gain}}^{\text{OCHM}} = \frac{C_{\text{OCHM}} - C_{\text{MSC}}}{C_{\text{MSC}}} \tag{36}$$

where C_{OCHM} and C_{MSC} indicate the user capacity of the OCHM-based system and that of the MSC-based system, respectively. Fig. 8 shows the capacity gain of the OCHM-based system over the MSC-based system. In Fig. 8, a GH scheme is selected as an HP generation method in the OCHM system. When an omnidirectional antenna is used at the BS, the capacity gain increases as the channel activity decreases. If η and the channel activity are set at 0.6 and 0.1, respectively, the capacity gain $C_{\text{gain}}^{\text{OCHM}}$ with CC and TC are equal to 23% and 37%,

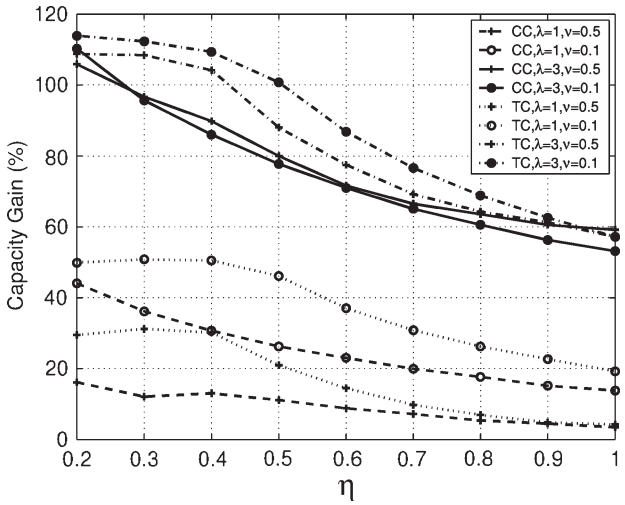

Fig. 8. Capacity gain of the OCHM-based system over the MSC-based system.

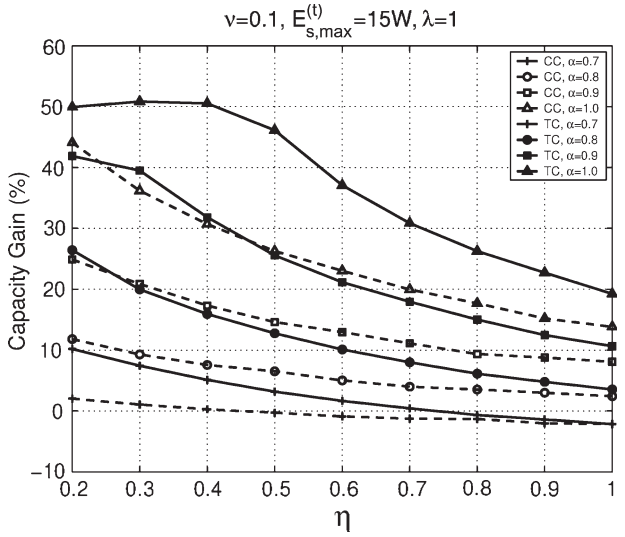

Fig. 9. Capacity gain of the OCHM-based system over the MSC-based system for varying orthogonality factors.

respectively. When a 3-sector antenna is used at the BS, the capacity gain is much larger than that with an omnidirectional antenna. When a 3-sector antenna is used at the BS, η is set at 0.6, and the channel activity is 0.1. The $C_{\text{gain}}^{\text{OCHM}}$ with a CC and a TC are equal to 71% and 87%, respectively. The capacity gain increases as we use a more powerful channel coding scheme, since the additional energy decreases at an MS in the OCHM-based system. Thus, the TC is a more attractive coding scheme in the OCHM-based system. Furthermore, the capacity gain decreases as the other-cell interference increases.

So far, we have assumed that α is equal to 1; i.e., orthogonality is perfectly restored among orthogonal codes. In real environments, the orthogonality factor varies according to varying channels. Fig. 9 shows the capacity gain of the OCHM-based system over the MSC-based system for varying the orthogonality factor α. The OCHM-based system is more sensitive to the orthogonality factor than the MSC-based system, because all active users in the OCHM-based system induce the inner-cell interference due to multipath fading. In the MSC-based system, the active users in the same code set induce the inner-cell interference due to multipath fading, whereas the active users in the different code set induce only the inner-cell interference due to the nonzero correlation between different code sets, which is independent of the orthogonality factor. The OCHM-based system yields better performance than the MSC-based system in most situations, although the capacity gain decreases as the orthogonality factor decreases.

VI. Conclusion

In this paper, we have compared both the OCHM- and the MSC-based systems, which have been proposed to accommodate more users than the maximum number of available orthogonal codes in the CDMA downlink. The OCHM-based system does not induce inner-cell interference. However, it requires more energy at an MS to compensate for the information loss at a BS. The MSC-based system uses nonorthogonal sequences that involve inner-cell interference to improve the downlink user capacity. Numerical examples show that the OCHM-based system can accommodate more users than the MSC-based system. The capacity gain of OCHM-based system increases as the other-cell interference decreases and the channel activity decreases. Thus, the OCHM-based system is a more effective scheme than the MSC-based system, considering that a code-limited situation occurs more frequently in the case of low other-cell interference and low channel activity. However, the OCHM-based system is more sensitive to the orthogonality factor. Note that we have used a POM for the received signal model in the OCHM-based system. The POM provides the lower bound of BER performance so that the OCHM-based system can be better if we consider the synergy effect at the MS. We have left the performance comparison between OCHM-based systems and TDM-based scheduling systems for further study.

References

[1] *Physical Layer Aspects of UTRA High Speed Downlink Packet Access (Release 4)*, Mar. 2001. 3GPP TR25.848 V4.0.0.
[2] *cdma2000 High Rate Packet Data Air Interface Specification*, Oct. 2000. 3GPP2. C.S0024 v.4.0.
[3] T. Ikeda, S. Sampei, and N. Morinaga, "TDMA-based adaptive modulation with dynamic channel assignment for high-capacity communication systems," *IEEE Trans. Veh. Technol.*, vol. 49, no. 2, pp. 404–412, Mar. 2000.
[4] R. Tafazolli, *Technologies for the Wireless Future; Wireless World Research Forum (WWRF)*. Hoboken, NJ: Wiley, 2005.
[5] WINNER, *Final Report on Identified RI Key Technologies, System Concept, and Their Assessment*, Dec. 2005. D2.10 v1.0.
[6] H. Ekstrom, A. Furuskar, J. Karlsson, M. Meyer, S. Parkvall, J. Torsner, and M. Wahlqvist, "Technical solutions for the 3G long-term evolution," *IEEE Commun. Mag.*, vol. 44, no. 3, pp. 38–45, Mar. 2006.
[7] WiMAX Forum Website. [Online]. Available: http://www.wimaxforum.org/
[8] S. Park and D. K. Sung, "Orthogonal code hopping multiplexing," *IEEE Commun. Lett.*, vol. 6, no. 12, pp. 529–531, Dec. 2002.
[9] J. K. Kwon, S. Park, and D. K. Sung, "Log-likelihood ratio (LLR) conversion schemes in orthogonal code hopping multiplexing," *IEEE Commun. Lett.*, vol. 7, no. 3, pp. 104–106, Mar. 2003.
[10] J. H. Chung, S. Park, and D. K. Sung, "Symbol perforation reduction schemes for orthogonal code hopping multiplexing," *IEICE Trans. Commun.*, vol. E88-B, no. 10, pp. 4107–4111, Oct. 2005.

[11] S. H. Moon, S. Park, J. K. Kwon, and D. K. Sung, "Capacity improvement in CDMA downlink with orthogonal code-hopping multiplexing," *IEEE Trans. Veh. Technol.*, vol. 55, no. 2, pp. 510–527, Mar. 2006.
[12] J. K. Kwon, S. Park, and D. K. Sung, "Collision mitigation by log-likelihood ratio (LLR) conversion in orthogonal code-hopping multiplexing," *IEEE Trans. Veh. Technol.*, vol. 55, no. 2, pp. 709–717, Mar. 2006.
[13] E. A. Geraniotis and M. B. Pursley, "Error probabilities for slow-frequency-hopped spread-spectrum multiple-access communications over fading channels," *IEEE Trans. Commun.*, vol. COM-30, no. 5, pp. 996–1009, May 1982.
[14] S. H. Moon, J. Kim, and D. K. Sung, "Performance analysis of orthogonal frequency and code hopping multiplexing," *IEEE Trans. Wireless Commun.*, vol. 6, no. 10, pp. 3803–3815, Oct. 2007.
[15] J. K. Kwon, S. Park, D. K. Sung, and M. G. Kyeong, "Performance comparison of orthogonal code hopping multiplexing (OCHM) and HDR schemes in synchronous downlink," in *Proc. IEEE WCNC*, Mar. 2002, pp. 2000–2005.
[16] K. Yang, Y.-K. Kim, and P. V. Kumar, "Quasi-orthogonal sequences for code-division multiple-access systems," *IEEE Trans. Inf. Theory*, vol. 46, no. 3, pp. 982–993, May 2000.
[17] *3GPP, Third Generation Partnership Project: Technical Specification Group Radio Access Network*, Jun. 2001. 3GPP TS 25 series.
[18] *TIA/EIA, Physical Layer Standard for cdma2000 Spread Spectrum Systems*, Jun. 15, 2001. 3GPP2 C.S0002 Ver. 3.0.
[19] L. Korowajczk *et al.*, *Designing cdma2000 Systems*. Hoboken, NJ: Wiley, 2004.
[20] A. G. Shanbhag, "Optimal QPSK modulated quasi-orthogonal functions for IS-2000," in *Proc. IEEE 6th Int. Symp. Spread Spectrum Tech. Appl.*, Sep. 2000, vol. 2, pp. 756–760.
[21] J. O. Carnero, K. I. Pederson, and P. E. Mogensen, "Capacity gain of an uplink-synchronous WCDMA system under channelization code constraints," *IEEE Trans. Veh. Technol.*, vol. 53, no. 4, pp. 982–991, Jul. 2004.
[22] S. Tsai, F. Khaleghi, S. J. Oh, and V. Vanghi, "Allocation of Walsh codes and quasi-orthogonal functions in cdma2000 forward link," in *Proc. IEEE VTC—Fall*, Oct. 2001, vol. 2, pp. 747–751.
[23] S. H. Moon, J. K. Kwon, J. Kim, and D. K. Sung, "Group mode hopping for collision mitigation in orthogonal code hopping multiplexing," *IEEE Trans. Veh. Technol.*, Sep. 2008, to be published.
[24] B. C. Jung, H. Jin, D. K. Sung, and S. Y. Chung, "Performance analysis of orthogonal code hopping multiplexing systems," in *Proc. IEEE ICC*, Jun. 2006, vol. 5, pp. 2078–2082.
[25] A. J. Viterbi, "Convolutional codes and their performance in communication systems," *IEEE Trans. Commun.*, vol. COM - 19, no. 5, pp. 751–772, Oct. 1971.
[26] C. Berrou, A. Glavieux, and P. Thitimajshima, "Near Shannon limit error-correcting coding and decoding: Turbo-codes," in *Proc. IEEE ICC*, May 1993, pp. 1064–1070.
[27] S. Benedetto and G. Montorsi, "Unveiling turbo codes: Some results on parallel concatenated coding schemes," *IEEE Trans. Inf. Theory*, vol. 42, no. 2, pp. 409–428, Mar. 1996.
[28] S. Benedetto and G. Montorsi, "Design of parallel concatenated convolutional codes," *IEEE Trans. Commun.*, vol. 44, no. 5, pp. 591–600, May 1996.
[29] L. C. Perez, J. Seghers, and D. J. Costello, Jr., "A distance spectrum interpretation of turbo codes," *IEEE Trans. Inf. Theory*, vol. 42, no. 6, pp. 1698–1709, Nov. 1996.
[30] R. Garello, P. Pierleoni, and S. Benedetto, "Computing the free distance of turbo codes and serially concatenated codes with interleavers: Algorithms and applications," *IEEE J. Sel. Areas Commun.*, vol. 42, no. 6, pp. 1698–1709, Nov. 1996.
[31] Turbo Code Website. [Online]. Available: http://www.tlc.polito.it/garello/turbodistance/turbodistance.html
[32] S. Burger, H. Buddendick, and G. Wolfie, "Location dependent CDMA orthogonality in system level simulations," in *Proc. IEEE VTC—Spring*, May 2005, vol. 1, pp. 419–423.
[33] S. S. Cho, B. C. Jung, and D. K. Sung, "Capacity analysis of downlink CDMA systems with quasi-orthogonal sequences," in *Proc. IEEE GLOBECOM*, Nov. 2006, pp. 1–6.
[34] J. S. Lee and L. E. Miller, *CDMA Systems Engineering Handbook*. Norwood, MA: Artech House, 1998.
[35] J. Conan, "The weight spectra of some short low-rate convolutional codes," *IEEE Trans. Commun.*, vol. COM-32, no. 9, pp. 1050–1053, Sep. 1984.

Bang Chul Jung (S'02–M'08) received the B.S. degree in electronics engineering from Ajou University, Suwon, Korea, in 2002 and the M.S. and Ph.D. degrees in electrical and computer engineering from the Korea Advanced Institute of Science and Technology (KAIST), Daejeon, Korea, in 2004 and 2008, respectively.

Since January 2008, he has been a Senior Research Engineer with the Institute for Information Technology Convergence, KAIST. His research interests include orthogonal resource hopping systems for packet data transmission, OFDM systems, radio resource management, wireless scheduling algorithms, information theory, link- and system-level simulations for 4G wireless communication systems, adaptive modulation and coding, and MIMO systems.

Dr. Jung received the Bronze Prize at the Intel Student Paper Contest in 2005.

Sung Soo Cho received the B.S. degree in electrical and electronics engineering from Kyungpook National University, Daegu, Korea, in 2004 and the M.S. degree in electrical and computer engineering from the Korea Advanced Institute of Science and Technology, Daejeon, Korea, in 2006.

Since January 2006, he has been a Research Engineer with the QoS Control Platform Division, KT, Daejeon, where he has been developing QoS manager systems. His research interests include policy and charging control architecture in WiMAX/3GPP systems, orthogonal resource hopping systems for packet data transmission, radio resource management, and quality-of-service issues for voice-over Internet Protocol and voice-on-demand services in wireless systems.

Dan Keun Sung (S'80–M'86–SM'00) received the B.S. degree in electronics engineering from the Seoul National University, Seoul, Korea, in 1975 and the M.S. and Ph.D. degrees in electrical and computer engineering from the University of Texas, Austin, in 1982 and 1986, respectively.

From May 1977 to July 1980, he was a Research Engineer with the Electronics and Telecommunications Research Institute (ETRI), where he was engaged in various projects, including the development of an electronic switching system. In 1986, he joined the faculty of the Korea Advanced Institute of Science and Technology (KAIST), Daejeon, Korea, where he is currently a Professor with the Department of Electrical Engineering and Computer Science. From 1996 to 1999, he was the Director of the Satellite Technology Research Center (SaTReC), KAIST. He was the Division Editor of the *Journal of Communications* and *Networks*. His research interests include mobile communication systems and networks, high-speed networks, next-generation IP-based networks, traffic control in wireless and wireline networks, signaling networks, intelligent networks, performance and reliability of communication systems, and microsatellites.

Dr. Sung is a member of the Institute of Electrical, Information, and Communication Engineers, Korea Information and Communications Society, Phi Kappa Phi, and Tau Beta Pi. He is the Editor of *IEEE Communications Magazine*. He was the Vice Chair of the 2002 IEEE International Conference on (ICC) Symposium on Global Service Portability and Infrastructure for Next-Generation Virtual Home and Office Environments and a Program Cochair of the 2002 Globecom Symposium on Service Infrastructure for Virtual Enterprise Environments. He was also the General Conference Chair and the Vice Chair of Technical Program Committee of ICC 2005. He received National Order of Merits, the Dongbaek Medal in 1992, the Research Achievement Award in 1997, the MoMuc Paper Award in 1997, the Academic Excellence Award in 2000, the Best Paper Award at the Sixth Asia-Pacific Conference on Communications (APCC 2000), and This Month's Scientist Award from the Ministry of Science and Technology (MOST) and Korea Science and Engineering Foundation (KOSEF) in 2004.